Quinoxaline-Containing Polyfluorenes: Synthesis, Photophysics, and Stable Blue Electroluminescence

Abhishek P. Kulkarni, Yan Zhu, and Samson A. Jenekhe*

Departments of Chemical Engineering and of Chemistry, University of Washington, Seattle, Washington 98195

Received September 13, 2004; Revised Manuscript Received December 4, 2004

ABSTRACT: Six new copolymers of 9,9′-dioctylfluorene and 2,3-bis(*p*-phenylene)quinoxaline were synthesized, characterized, and used as blue-emitting materials in light-emitting diodes (LEDs). The glass transition temperature increased from 67 °C in poly(9,9′-dioctylfluorene) (PFO) to as high as 160 °C in the alternating copolymer. All the copolymers emitted blue light in dilute toluene solution (417−423 nm), with photoluminescence (PL) quantum yields that decreased from 72% to 26% with increasing quinoxaline content, and as thin films (429−439 nm). The PL lifetimes of solutions and thin films were 308−617 ps. Blue electroluminescence with Commission Internationale de L'Eclairage coordinates of (0.16, 0.06) was achieved. Luminances of 240−520 cd/m^2 varied with the quinoxaline content. External quantum efficiencies of up to 1% at brightnesses of over 100 cd/m^2 were obtained. Enhancement in LED performance by factors of 3−6 compared to that of PFO was achieved in a copolymer containing 5 mol % 2,3-bis(*p*-phenylene)quinoxaline. Significant enhancements in LED brightness and external quantum efficiency by factors of up to 120 were observed in copolymers containing 15−50 mol % 2,3-bis(*p*-phenylene)-quinoxaline when using bilayer LiF/Al cathodes instead of Al. These results demonstrate that composition can be used to optimize the light-emitting properties of electroluminescent copolymers and that the fluorene−quinoxaline copolymers are useful materials for developing stable blue LEDs.

Introduction

Organic light-emitting diodes (OLEDs) based on organic semiconductors and conjugated polymers have attracted much attention as candidates for the next generation of full-color flat panel displays.[1−13] OLED displays in consumer products such as cell phones and digital cameras are already on the market. Achievement of stable blue electroluminescence with high external quantum efficiency (EQE) remains an important challenge on the path toward full color polymer displays. Polyfluorenes have emerged as very promising materials for blue emission due to their unique combination of high thermal stability, high hole mobilities, easy processability, and high photoluminescence (PL) quantum yields in the solid state.[5,6] However, a major problem in using the poly(9,9′-dialkylfluorene)s as blue-emitting materials in OLEDs is the undesirable lower energy emission band centered at 530−540 nm that appears under device operation, turning the pure blue emission to blue-green color.[5a,b,7] Many approaches to stabilize the pure blue emission from the polyfluorenes have been explored with varying degrees of success.[8,9] Due to their high PL quantum yields, polyfluorenes have been copolymerized with a host of other comonomers, both p-type and n-type, to tune the emission color or enhance the charge-injection and -transport properties in the predominantly p-type poly(9,9′-dioctylfluorene) (PFO) backbone.[10−13] Fluorene-containing polymers have been shown to emit efficiently across the entire visible spectrum.[1d,e]

Blue-emitting PFO is a p-type material that transports holes with high mobility.[6] However, electron injection and transport in PFO is poor. Our motivation for the present work was to synthesize polyfluorenes with improved electron-injection and -transport characteristics by copolymerizing with an electron-deficient (n-type) building block while retaining the blue emission, with the aim of achieving stable blue OLEDs with high brightness and EQE. One of the challenges of this approach is to improve the electron-transport properties while preserving the desired pure blue emission and high luminescence quantum yields. We point out that such an approach to improving the electron-transport ability of blue-emitting polyfluorenes has also been employed previously by using n-type building blocks such as oxadiazole,[12a] quinoline,[12b] pyridine,[12c] and quinoxaline,[12b,13] either in the main chain or as pendants to the polyfluorene backbone. However, studies of the variation in electroluminescence of the copolymers as a function of the copolymer composition were not performed, except in the recently reported fluorene−pyridine copolymers.[12c] Systematic investigations of such structure−property relationships of polyfluorene copolymers are essential for a full understanding of the role of a particular n-type moiety. We chose quinoxaline as the n-type building block since it is known to have a high electron affinity and good thermal stability and has been successfully incorporated in polymers for use as electron-transport materials in multilayer OLEDs.[14,15] While there are a few previous reports on quinoxaline-containing copolymers based on p-type emissive polymers such as polyfluorene[12b,13] and poly(*p*-phenylenevinylene) (PPV),[16] only alternating quinoxaline−fluorene copolymers were reported,[12b,13] and poor OLED performance (0.013% EQE) was obtained using them as blue emissive materials.[13b] Additionally, the prior alternating quinoxaline−fluorene copolymers contained linear rodlike 6,6′-bis(3-phenylquinoxaline) units in the main chain, whereby the resultant thin film blue emission had emission maxima at 455−460 nm with poor Commission Internationale de L'Eclairage (CIE) coordinates.[12b,13]

* To whom correspondence should be addressed. E-mail: jenekhe@u.washington.edu.

10.1021/ma048118d CCC: $30.25
Published on Web 02/02/2005

Chart 1

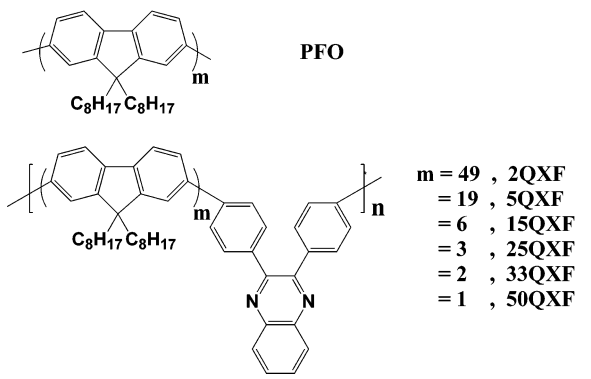

In this paper, we report the synthesis, photophysics, and electroluminescence of a series of six new 2,3-bis(*p*-phenylene)quinoxaline-containing poly(9,9′-dioctylfluorene)s (QXFs) where the quinoxaline unit is attached such that the polyfluorene backbone is kinked, thereby improving the chance of retention of blue emission with deep blue CIE coordinates. A series of polyfluorene copolymers containing 2, 5, 15, 25, 33, and 50 mol % quinoxaline, denoted 2QXF, 5QXF, 15QXF, 25QXF, 33QXF, and 50QXF (Chart 1), respectively, were synthesized by Suzuki coupling reaction and systematically investigated. Structure−property relationships of the copolymers were investigated by differential scanning calorimetry (DSC), optical absorption, steady-state PL, time-resolved PL decay dynamics, PL quantum yield measurements, and electroluminescence. Systematic trends in the variation of relevant copolymer properties such as the glass transition temperature and PL quantum yields were observed. Bright blue electroluminescence (EL) was obtained from the QXF copolymers, demonstrating that they can be used as stable blue electroluminescent materials in polymer LEDs.

Experimental Section

Materials. All starting materials and reagents were purchased from Aldrich and used without further purification. 2,3-Bis(4-bromophenyl)quinoxaline was prepared according to the literature method.[16]

Polymerization. The following general procedure was used for the preparation of all the copolymers and PFO homopolymer. To a three-necked flask were added 9,9-dioctylfluorene 2,7-bis(trimethyleneboronate) (558.4 mg, 1 mmol), 2,7-dibromofluorene and 2,3-bis(4-bromophenyl)quinoxaline (total 1 mmol), Aliquat 336 (122.4 mg), and toluene (15 mL). Once all the monomers were dissolved, 2 M aqueous sodium carbonate solution (10 mL) was added. The flask equipped with a condenser was then evacuated and filled with argon several times to remove traces of air. $Pd(PPh_3)_4$ (15 mg, 0.013 mmol) was then added under an argon atmosphere. The mixture was then stirred for 48 h at 110 °C under argon. The reaction mixture was cooled to room temperature, and the organic layer was separated, washed with water, and precipitated into methanol. The crude polymer was filtered, washed with excess methanol, and dried. The fibrous polymer was purified by a Soxhlet extraction in acetone for 2 days. The resultant polymer was further purified by being dissolved in THF and reprecipitated into methanol several times. The pure copolymers were obtained after drying under vacuum at 50 °C overnight (yield 68−75%).

PFO Homopolymer. ^{1}H NMR ($CDCl_3$): δ (ppm) 7.85 (br, 2H), 7.70 (br, 4H), 2.15 (br, 4H), 1.16 (br, 20H), 0.84 (m, 10H). FT-IR (film, cm^{-1}): 3019, 2926, 2853, 1459, 1253, 885, 813, 756.

50QXF Copolymer. ^{1}H NMR ($CDCl_3$): δ (ppm) 8.24 (br, 2H), 7.65−7.80 (m, 16H), 2.08 (br, 4H), 1.10−1.20 (m, 20H), 0.80 (m, 10H). FT-IR (film, cm^{-1}): 3060, 3033, 2926, 2853, 1607, 1532, 1464, 1398, 1344, 1249, 1220, 1059, 1016, 977, 819, 760, 604.

Other copolymers showed NMR and FT-IR spectra similar to those of 50QXF copolymer except that the relative intensities of the signals are different due to the different composition of the copolymer. 2QXF showed an NMR spectrum similar to that of PFO homopolymer due to the low concentration of quinoxaline moiety.

Characterization. FT-IR spectra were taken on a Perkin-Elmer 1720 FTIR spectrophotometer with NaCl plates. ^{1}H NMR spectra were recorded on a Bruker-DRX499 at 500 MHz. Gel permeation chromatography (GPC) analysis of the polymers was performed on a Waters gel permeation chromatograph with Shodex gel columns and Waters model 150 C refractive index detectors using THF as eluent and polystyrene standards as reference. DSC analysis was performed on a TA Instrument Q100 differential scanning calorimeter under N_2 at a heating rate of 10 °C/min, and thermogravimetric analysis (TGA) was conducted with a TA Instrument Q50 thermogravimetric analyzer at a heating rate of 20 °C/min under a nitrogen gas flow. UV−vis absorption spectra were recorded on a Perkin-Elmer model Lambda 900 UV/vis/near-IR spectrophotometer. The PL emission spectra were obtained with a Photon Technology International (PTI) Inc. model QM-2001-4 spectrofluorimeter.

To measure the PL quantum yields (Φ_f), polymer solutions in spectral grade toluene were prepared. The concentration ($\sim 10^{-5}$ M) was adjusted so that the absorbance of the solution would be lower than 0.1. A 10^{-5} M solution of 9,10-diphenylanthracene in toluene ($\Phi_f = 0.93$) was used as a standard.[17]

Time-Resolved Photoluminescence Decay Dynamics. Fluorescence decays of the copolymers in solution and thin films were obtained on a PTI model QM-2001-4 spectrofluorimeter equipped with a Strobe Lifetime upgrade. The instrument utilizes a nanosecond flash lamp filled with a high-purity nitrogen/helium (30:70 v/v) mixture as the excitation source and a stroboscopic detection system. The decay curves were analyzed using a software package provided by the manufacturer. Reduced χ^2 values, Durbin−Watson parameters, and weighted residuals were used as the goodness-of-fit criteria. All measurements were done in ambient conditions at room temperature.

Fabrication and Characterization of LEDs. Indium−tin oxide (ITO) coated glass substrates (Delta Technologies Ltd., Stillwater, MN) were cleaned sequentially in ultrasonic baths of a 2-propanol/deionized water (1:1 volume) mixture, toluene, deionized water, and acetone, and then dried at 60 °C in a vacuum overnight. A 50 nm thick hole-injection layer of poly(ethylenedioxythiophene) doped with poly(styrenesulfonate) (PEDOT) was spin-coated on top of ITO from a ~1 wt % dispersion in water and dried at 200 °C for 15 min under a vacuum. Poly(*N*-vinylcarbazole) (PVK) (Scientific Polymer Products, Inc., Ontario, NY) was used as a hole-transport layer. Thin films (~15 nm) of PVK were deposited onto the PEDOT layer by spin-coating from 1 wt % solutions in toluene and dried in a vacuum at 60 °C for at least 8 h. Each QXF copolymer solution in toluene was made at a concentration of 10 mg/mL and then filtered through a 0.2 μm syringe filter. Thin films (50 nm) of the copolymers were spin-coated from these solutions onto the PVK layer and dried at 60 °C in a vacuum overnight. Due to the solubility of PVK in toluene, it is likely that the interface between the PVK and copolymer layers is diffuse rather than being flat and well-defined. However, overall film thicknesses of PVK + copolymer were ca. 60−70 nm, which were measured by an Alpha-Step 500 surface profiler (KLA Tencor, Mountain View, CA). The substrates were then transferred to an AUTO 306 vacuum coater (BOC Edwards, Wilmington, MA), and 2 nm of LiF was deposited from a molybdenum boat through a shadow mask onto the polymer films. Finally, a 130−150 nm thick layer of Al was evaporated without breaking the vacuum, typical

Scheme 1

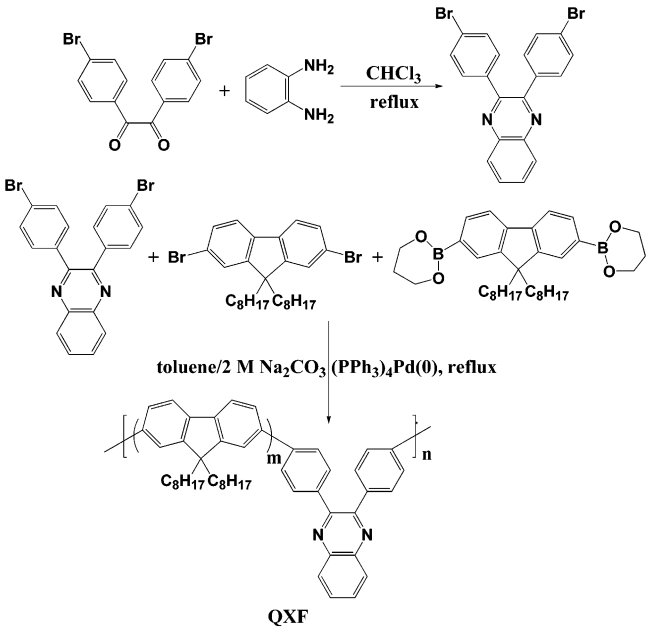

evaporations being done at base pressures lower than 2×10^{-6} Torr. The resultant active area of each EL device was 0.2 cm^2.

EL spectra were obtained using a PTI QM-2001-4 spectrophotometer. Current−voltage characteristics of the LEDs were measured using an HP4155A semiconductor parameter analyzer (Yokogawa Hewlett-Packard, Tokyo). The luminance was simultaneously measured using a model 370 optometer (UDT Instruments, Baltimore, MD) equipped with a calibrated luminance sensor head (model 211) and a 5× objective lens. The device external quantum efficiencies were calculated using procedures reported previously.[2a,7f,9a] All the device fabrication and characterization steps were done under ambient laboratory conditions.

Results and Discussion

Synthesis and Characterization. The synthetic procedures used to prepare the monomer and polymers are outlined in Scheme 1. The condensation of 4,4′-dibromobenzil with 1,2-phenylenediamine afforded the monomer 2,3-bis(4-bromophenyl)quinoxaline with high yield (68%).[16] Random and alternating poly(9,9-dioctylfluorene-*co*-quinoxaline) (QXF) copolymers were synthesized by Suzuki coupling polymerization. The molar ratio of quinoxaline moiety in the copolymers was controlled by adjusting the molar ratio between 9,9′-dioctyl-2,7-dibromofluorene and 2,3-bis(4-bromophenyl)-quinoxaline while maintaining a 1:1 molar ratio between the dibromides and the bis(trimethyleneboronate). The corresponding polyfluorene homopolymer, PFO, was also prepared under the same conditions for comparison. All the copolymers were soluble in organic solvents such as chloroform, toluene, and tetrahydrofuran (THF). The number-average molecular weights (M_n) of these polymers were determined by GPC against polystyrene standards to be 7100−31900 with a polydispersity index of 1.88−2.68 (Table 1).

The chemical structures of the polymers were verified by ^{1}H NMR and FT-IR spectra. The ^{1}H NMR spectra of the copolymers and PFO homopolymer were in good agreement with the structures of the polymers. Representative ^{1}H NMR spectra of copolymer 50QXF and PFO homopolymer are shown in Figure 1. A small peak at 8.24 ppm due to the two protons (labeled "o" in Figure 1) near nitrogen atoms in the quinoxaline unit was

Table 1. Molecular Weights and Thermal Properties of Polymers

polymer	M_n [a]	M_w/M_n [a]	T_g [b] (°C)	T_d [c] (°C)
PFO	23200	2.68	67	458
2QXF	31900	2.08	67	460
5QXF	25300	2.56	69	459
15QXF	16800	2.40	91	457
25QXF	12800	2.58	116	460
33QXF	11300	2.48	125	455
50QXF	7100	1.88	160	457

[a] Molecular weights were determined by GPC using polystyrene standards. [b] Glass transition temperature. [c] Onset decomposition temperature measured by TGA under nitrogen.

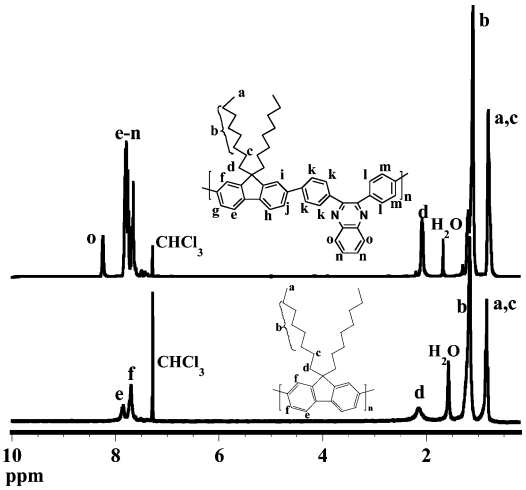

Figure 1. ^{1}HNMR spectra of PFO homopolymer and 50QXF copolymer.

observed in the spectra of all the copolymers except 2QXF, where the concentration of the quinoxaline moiety was too low. The multiple peaks in the range of 7.65−7.80 ppm correspond to the other aromatic protons in the quinoxaline and fluorene units. The resonances at 2.08, 1.10, and 0.80 ppm are assigned to the aliphatic protons in the octyl chains. FT-IR spectra of these copolymers and PFO homopolymer also confirmed their molecular structures. Representative FT-IR spectra of copolymer 50QXF and PFO homopolymer are shown in Figure 2. Compared to PFO homopolymer, the new vibrational bands at 1607 and 1532 cm^{-1} in all the copolymers are due to stretching vibrations of the C=N group in the quinoxaline ring.

The thermal properties of the polymers were evaluated by TGA and DSC, and the results are summarized in Table 1. TGA revealed that the onset decomposition temperatures of the copolymers and PFO homopolymer under nitrogen were in the range of 455−460 °C, indicative of good thermal stability. The DSC second-heating scans of the copolymers and PFO homopolymer are shown in Figure 3. PFO homopolymer exhibits three transitions: a glass transition (T_g = 67 °C), a crystallization exothermic peak (94 °C), and a melting peak (152 °C). These typical thermal characteristics in PFO are similar to those of previous reports.[8b,18] Similar thermally induced phase transitions were observed for copolymer 2QXF, but were not as well resolved as in PFO. The DSC traces of all the other copolymers containing greater than 2 mol % quinoxaline showed no crystallization or melting peaks, but only glass transitions. The glass transition temperatures of these copolymers are in the range of 69−160 °C, increasing

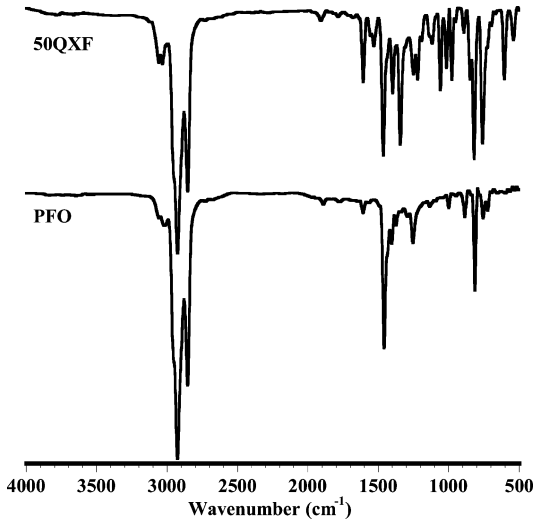

Figure 2. FT-IR spectra of PFO homopolymer and 50QXF copolymer.

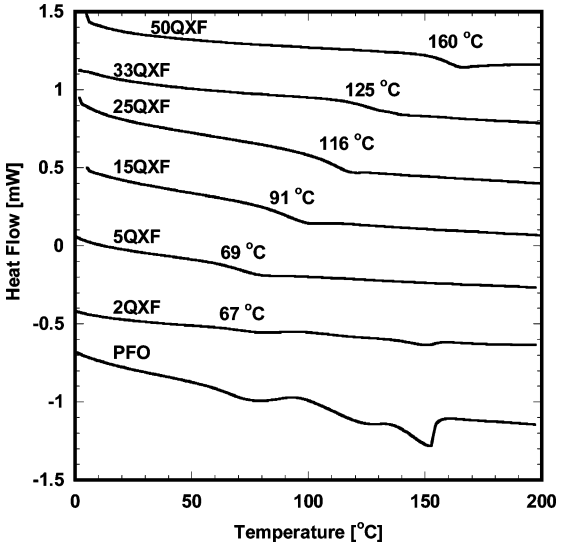

Figure 3. Second-heating DSC curves of the polymers with a heating rate of 10 °C/min in nitrogen.

steadily from the 67 °C T_g in PFO to 160 °C in 50QXF. This clearly indicates that the incorporation of the rigid quinoxaline unit into the polyfluorene backbone reduces the segmental mobility and effectively suppresses the tendency of the polymer chains to densely pack and crystallize. This improved thermal resistance of the copolymers bodes well for stable blue emission from LEDs made from them.

Photophysical Properties. The normalized optical absorption and PL emission spectra of the PFO homopolymer and the six copolymers in dilute (10^{-5} M) toluene solution are shown in Figure 4. PFO has an absorption maximum at 388 nm corresponding to the $\pi-\pi^*$ transition of the polyfluorene backbone. All the quinoxaline-containing copolymers have blue-shifted absorption maxima compared to PFO. The absorption maximum is progressively blue shifted with increasing quinoxaline content, from 383 nm in 2QXF to 365 nm in 50QXF. The full width at half-maximum (fwhm) of the absorption spectra increases with increasing quinoxaline content, suggesting greater inhomogeneous broadening due to the local disorder induced by the presence of kinked 2,3-bis(*p*-phenylene)quinoxaline linkages. The gradual blue shift in the absorption maxima

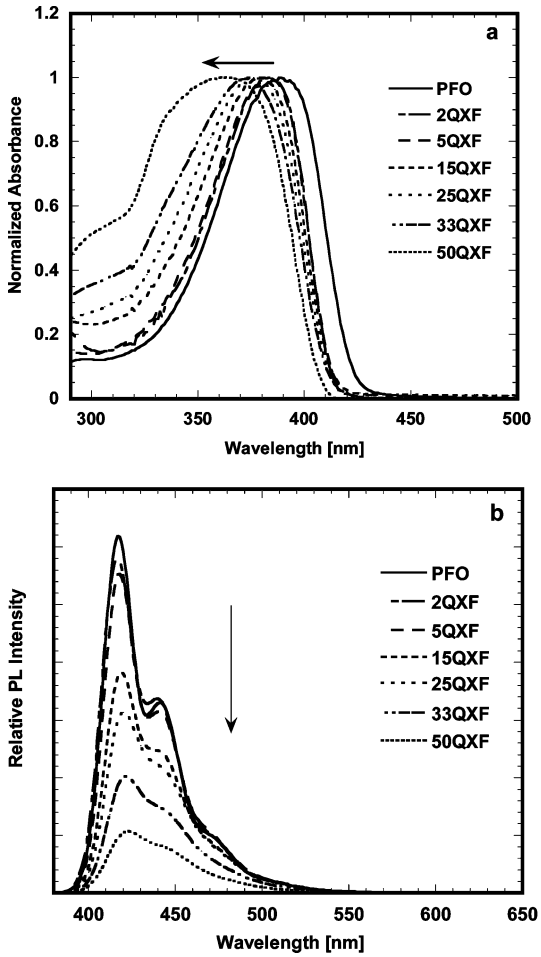

Figure 4. (a) Normalized optical absorption spectra of 10^{-5} M solutions of PFO and QXF copolymers in toluene. (b) PL emission spectra of 10^{-5} M solutions of the polymers in toluene. The excitation wavelength was 380 nm.

of the copolymers suggests increased disruption of π-conjugation caused by the increasing amounts of the bent 2,3-bis(*p*-phenylene)quinoxaline linkages in the PFO backbone. Also, the absorption onsets of the spectra shift to higher energy in going from 2QXF to 50QXF, indicating shortened conjugation lengths. The incorporation of such kinked linkages in polymer backbones has been used successfully in poly(*p*-phenylenevinylene) backbones to control the conjugation length of the polymer and tune the emission colors.[19]

The PL emission spectra under 380 nm excitation of PFO and the copolymers in dilute toluene solution are shown in Figure 4b. The PFO emission spectrum has the typical vibronic progression with the 0−0 PL emission band located at 417 nm and the 0−1 transition at 440 nm.[5a] With increasing quinoxaline content, there is a slight red shift in the 0−0 emission band to 423 nm in 50QXF with simultaneous loss in vibronic structure of the emission spectra. However, the emission of all the copolymers remains blue. The 0−1 emission band at 440 nm in PFO becomes a shoulder in copolymers containing greater than 15 mol % quinoxaline. This loss of the well-resolved structure of the emission spectra in the copolymers suggests lack of intrachain ordering due to the many kinks in the copolymer backbone. The steady increase in Stokes shift from PFO to 50QXF suggests greater planarization of the backbone in the excited state due to intramolecular charge transfer in the donor−acceptor-type fluorene−quinoxaline copoly-

Table 2. Photophysical Properties of Polymers

polymer	$\lambda_{a,max}$[a] in solution (nm)	$\lambda_{f,max}$[b] in solution (nm)	Φ_f[c]	$\lambda_{a,max}$[a] in a thin film (nm)	$\lambda_{f,max}$[b] in a thin film (nm)
PFO	388	417	0.72	383	439
2QXF	383	417	0.69	382	439
5QXF	382	418	0.62	382	429
15QXF	379	419	0.48	380	431
25QXF	376	421	0.41	377	435
33QXF	373	422	0.35	374	436
50QXF	365	423	0.26	373	437

[a] The absorption maximum in toluene solution or in a thin film. [b] The PL emission maximum in toluene solution or in a thin film. [c] PL quantum yield in 10^{-5} M toluene solution.

mers.[20] The main photophysical properties of all the polymers are collected in Table 2.

Figure 5a shows the normalized optical absorption spectra of thin films of PFO and the six QXF copolymers after drying at 60 °C in a vacuum. The trends observed with increasing quinoxaline content in terms of the spectral shapes, peak positions, and fwhm are similar to those of the absorption spectra in dilute solution. PFO has an absorption maximum at 383 nm along with a distinct shoulder at ~430 nm. This absorption feature has been attributed to the β-phase of PFO, which is comprised of a sequence of intrachain ordered dioctylfluorene repeat units.[21] This low-energy transition completely disappears in the absorption spectra of all the QXF copolymers. This again confirms that the bent 2,3-bis(*p*-phenylene)quinoxaline linkages introduce disorder in the polyfluorene backbones and thus prevent ordered intrachain conformations. The distinct similarity between the thin film absorption spectra and the dilute solution spectra suggests comparable ground-state electronic structures of the QXF copolymers with no significant aggregation in the condensed state. Unlike the blue shift in the absorption onset observed in the solution spectra of the copolymers with increasing quinoxaline content, the absorption edges of the thin film spectra are all identical. This means that the same segments with extended delocalization are present in the copolymers in the solid state, giving rise to similar bulk electronic structures in all the copolymers. The optical band gaps derived from the absorption edge of the thin film spectra gave similar values of 2.9−3.0 eV for all copolymers.

Figure 5b shows the PL emission spectra of the copolymer thin films dried at 60 °C under 380 nm excitation. The PFO homopolymer spectrum shows the typical well-resolved vibronic structure with the 0−0 transition at 439 nm, followed by the 0−1 and 0−2 transitions at 464 and 493 nm, respectively.[5a] Copolymer 2QXF shows the 0−0 transition at 424 nm along with the dominant 0−1 transition at 439 nm. Further increase in the quinoxaline fraction in the copolymers results in a gradual loss of the vibronic structure, with the spectrum of 50QXF becoming broad enough to envelope the structured PFO emission spectrum. However, all the QXF copolymers retain the blue emission of the parent PFO backbone and are thus candidates for blue electroluminescence in LEDs.

The spectral instability in blue LEDs based on polyfluorenes under constant applied stress remains a continual problem.[5a,b,7] To test the stability of the quinoxaline copolymers toward thermal oxidation, the copolymer thin films were annealed at 200 °C in air for 1.5 h to accelerate degradation. The normalized emission spectra (with respect to the 0−0 emission band) of these annealed films are shown in Figure 5c. The PL emission spectrum of the PFO film dried at 60 °C is also shown for comparison. The annealed PFO film shows the signature broad green emission band at 530 nm, whose origin has been a subject of controversy in the literature.[7] The intensity of this broad low-energy emission band relative to the blue emission band steadily decreases with increasing quinoxaline content in the copolymer. Besides, the emission peak blue shifts

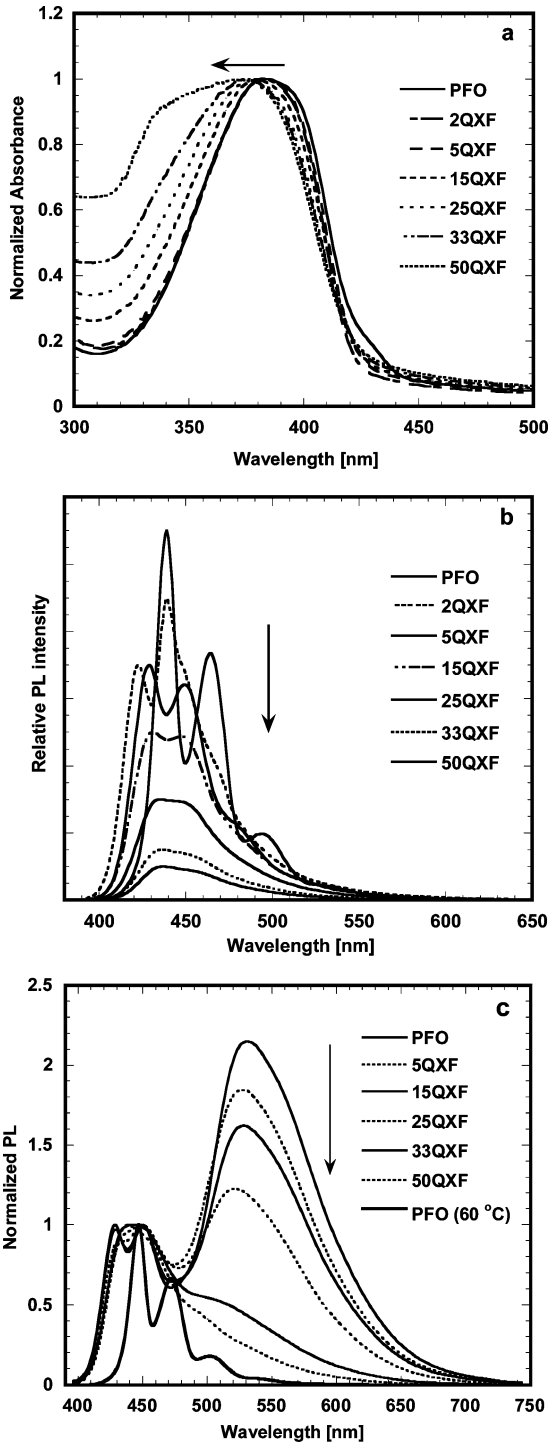

Figure 5. (a) Normalized optical absorption spectra of thin films of PFO and QXF copolymers. (b) PL emission spectra of the polymer thin films dried at 60 °C in a vacuum. (c) Normalized PL emission spectra (with respect to the 0−0 emission band) of the polymer thin films annealed at 200 °C in air for 1.5 h. The excitation wavelength was 380 nm.

from 530 nm in PFO to 521 nm in 25QXF, appearing only as a shoulder in the spectrum of 33QXF and almost disappearing in the 50QXF emission spectrum. Given the recent conclusive evidence that this additional green emission in polyfluorenes is from isolated fluorenone defects on the polyfluorene chains,[7c,f] the observed decrease in the intensity of the emission band suggests lower concentration of keto defects in the QXF copolymers. The electron-deficient quinoxaline moieties in the copolymers withdraw electron density from adjacent fluorene units and thereby reduce the susceptibility to oxidation at the C-9 position of the 9,9′-dioctylfluorene units. Given the increase in the T_g of the copolymers with increasing quinoxaline content (Table 1) and the lack of any crystallization/melt transitions in the quinoxaline copolymers (Figure 3), the copolymer thin films will be in a more disordered state relative to the PFO homopolymer thin film after the 200 °C heating and subsequent cooling to room temperature. This will minimize, but not completely eliminate, the interchain-assisted excitation energy migration to the fluorenone defects with increasing quinoxaline content in the copolymers. Thus, even if the same concentration of fluorenone defects are present in all the annealed copolymer thin films, the reduced interchain energy transfer to those defects could lead to the observed lower intensity of the fluorenone emission band in the high-T_g 50QXF copolymer versus the low-T_g 5QXF copolymer. The blue shift in the peak position of this fluorenone emission band could be a result of the variation in the local polarity of the medium surrounding the keto defect, which will vary depending on the quinoxaline fraction in the copolymer. Due to the strong polar character of the fluorenone emission band, significant red shifts have been observed in highly polar environments.[7f] Nonetheless, the improved spectral stability in the QXF copolymers relative to the PFO homopolymer augurs well for spectrally stable blue EL from LEDs made from the copolymers.

The fluorescence quantum yields (Φ_f) of all the polymers in dilute (10^{-5} M) toluene solution are listed in Table 2. The highest Φ_f value of 72% was observed for PFO homopolymer, with the Φ_f values steadily decreasing with increasing quinoxaline fraction in the copolymers. At low quinoxaline content, 2QXF and 5QXF, the Φ_f value remains high at 0.62−0.69. The lowest Φ_f value obtained was 26% for copolymer 50QXF. One likely reason for the decreasing Φ_f is the greater intramolecular charge transfer with increasing quinoxaline content.[20] Although solid-state Φ_f values were not calculated, the relative intensities in the thin film PL emission spectra suggested a trend in Φ_f values similar to that observed in solution. To further understand the nature of the emission from these quinoxaline-containing polyfluorenes, we investigated their fluorescence decays in both dilute solution and thin films as discussed next.

Time-Resolved PL Decay Dynamics. The fluorescence decay parameters of the polymers in solution and in thin films are collected in Table 3. The PL emission maximum of the copolymers was monitored in each case. In dilute toluene solution (10^{-5} M), the decay of the blue emission band for PFO and all the copolymers was found to be single-exponential, with lifetimes ranging from 421 to 617 ps. Given the lack of interchain interactions in dilute solution, this emission is assigned to intrachain singlet excitons on the polymer backbones. The observed lifetime of PFO homopolymer is comparable to the literature values, 520 ps.[22] With increasing quinoxaline content from 2QXF to 50QXF, the lifetime of the blue emission generally increases. Knowing the fluorescence quantum yields in dilute solution and these fluorescence lifetimes, the natural radiative lifetimes (τ_0) of the emission bands can be estimated. The τ_0 values were found to steadily increase in going from PFO (590 ps) to copolymer 50QXF (2.33 ns), suggesting slower radiative rate constants and increased channels for nonradiative decay. The increasing number of kinks in the QXF copolymer backbones with increasing quinoxaline fraction could be potential sites for efficient exciton quenching, leading to the observed steady decrease in Φ_f values (Table 2).

Table 3. Fluorescence Decay Lifetimes of Polymer Solutions and Thin Films[a]

polymer	fit[b]	τ_1 (nm) (A_1, %)	τ_2 (nm) (A_2, %)	χ^2	D−W[c]
		Solution			
PFO	F1	0.425		1.472	1.538
2QXF	F1	0.421		1.33	1.71
5QXF	F1	0.445		1.266	2.011
15QXF	F1	0.548		1.271	1.639
25QXF	F1	0.527		1.067	2.017
33QXF	F1	0.617		1.386	1.645
50QXF	F1	0.606		1.311	1.364
		Thin Film			
PFO	F1	0.394		1.376	1.526
2QXF	F2	0.395 (99.3)	2.37 (0.7)	1.304	1.611
5QXF	F2	0.373 (99.5)	2.97 (0.5)	1.798	1.316
15QXF	F2	0.339 (99.2)	2.78 (0.8)	1.272	1.48
25QXF	F2	0.528 (98.3)	3.22 (1.7)	2.6	1.19
33QXF	F2	0.448 (98.5)	2.95 (1.5)	1.313	1.579
50QXF	F2	0.308 (99.7)	4.04 (0.3)	0.998	1.823

[a] The excitation wavelength was 381 nm, and the PL emission maxima were monitored in each case. The concentration of all polymer solutions was 10^{-5} M in toluene. [b] F1 = single-exponential fit; F2 = biexponential fit. [c] Durbin−Watson parameter for the fits.

In going from the polymer dilute solutions to thin films, it is generally believed that interchain species such as aggregates or excimers play a more dominant role in the PL emission.[23] The fluorescence of a PFO homopolymer thin film was well-described by single-exponential decay with a short lifetime of 394 ps, slightly shorter than that in solution. The increased number of nonradiative decay sites such as polymer chain ends tends to generally reduce the lifetime in thin films. The lifetimes of the thin film QXF copolymers are also shorter than that in solution, ranging from 308 to 528 ps. However, the emissions are now described by biexponential decays, unlike the single-exponential fits in solution. Attempts to make single-exponential fits to the thin film decays gave very high χ^2 values of greater than 10. Biexponential decays led to substantially better fits to the data. For all copolymer thin films, the dominant emitting species had short lifetimes of less than 1 ns, which can be assigned to intrachain excitons. A very minor contribution (<2%) of a longer lived species with lifetimes ranging from ~2 to 4 ns is noted in all copolymers. Although unambiguous assignment of this 2−4 ns species is not possible, it is thought to be related to some interchain phenomenon such as aggregates. Nonetheless, the fact that more than 98% of the contribution to the blue emission comes from the short-lived species suggests that the degree of interchain interactions is minimal in thin films of the quinoxaline-containing polyfluorenes. Representative decay curves of copolymer 50QXF in toluene solution (10^{-5} M) and

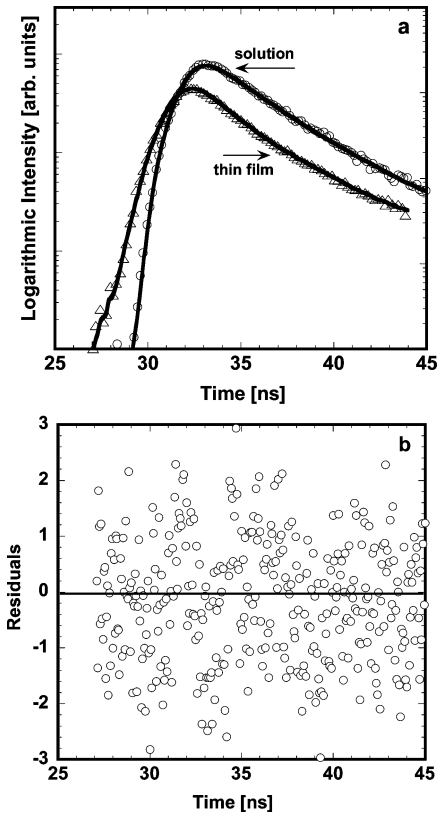

Figure 6. (a) Fluorescence decay curves of the PL emission peak of 50QXF in 10^{-5} M toluene solution and in a thin film with 381 nm excitation. Open symbols represent the actual data, and the solid lines are fits to the data. (b) Weighted residuals for the single-exponential fit corresponding to the solution decay curve.

in a thin film with the corresponding exponential fits are shown in Figure 6a along with the plot of weighted residuals for the fit (Figure 6b).

Electroluminescent Properties. Initial investigations of the EL properties of the quinoxaline-containing polyfluorenes were made by fabricating single-layer LEDs of the type ITO/PEDOT/polymer/Al. However, blue EL with poor performance was obtained with maximum brightness of only ~40−50 cd/m^2. Besides, there were a lot of nonemissive dark spots on the active area of the pixel in all cases, which led us to believe that doping of the QXF copolymers at the PEDOT/polymer interface caused significant quenching of the luminescence. Such charge-transfer and doping processes have been observed at the PEDOT interface.[24] It was thought that the addition of a buffer layer such as PVK which could also serve as a hole-transport/electron-blocking layer would help to mitigate this problem. Besides, the ionization potential (IP) of PFO is very large at 5.8 eV, leading to a substantial barrier for hole injection even from the PEDOT layer (ϕ = 5.2 eV). In the QXF copolymers, it is likely that the HOMO levels could be even lower lying due to the presence of the 2,3-bis(*p*-phenylene)quinoxaline groups. We investigated the electrochemical properties of the copolymers by cyclic voltammetry; however, no significant difference was observed between the redox waves of PFO and those of the QXF copolymers (not shown). Even for copolymer 50QXF, it was difficult to resolve any differences in either the oxidation or reduction waves, although it is expected that the quinoxaline groups would improve electron transport in the copolymers compared to PFO. This indicates that electron delocalization (conjugation) between the fluorene units and the 2,3-bis(*p*-phenylene)-quinoxaline moieties is poor due to the bent linkages in the current QXF copolymers.

Table 4. Device Characteristics of Type I LEDs: ITO/PEDOT/PVK/Polymer/Al

polymer	voltage (V)	current density (J, mA/cm^2)	brightness (L, cd/m^2)	CIE 1931 (x, y)[a]	EQE[b] (%)
PFO	15.6	500	190	(0.16, 0.06)	0.053
2QXF	10.3	336	300	(0.16, 0.06)	0.30
5QXF	16.4	500	560	(0.16, 0.05)	0.35
15QXF	17.3	500	150	(0.16, 0.07)	0.07
25QXF	14.5	500	60	(0.16, 0.05)	0.04
33QXF	9.2	240	12	(0.16, 0.07)	0.01
50QXF	9.4	312	2	(0.16, 0.08)	0.002

[a] The CIE coordinates are calculated at the maximum EQE. [b] The maximum EQE is calculated at the given voltage, current density, and brightness.

Table 5. Device Characteristics of Type II LEDs: ITO/PEDOT/PVK/Polymer/LiF/Al[a]

polymer	voltage (V)	current density (J, mA/cm^2)	brightness (L, cd/m^2)	CIE 1931 (x, y)[b]	EQE (%)
PFO	8.7 (7.1)	185 (46)	360 (106)	(0.16, 0.05)	0.60 (0.66)
2QXF	10.0 (9.1)	176 (87)	330 (180)	(0.16, 0.04)	0.72 (0.78)
5QXF	10.5 (9.0)	207 (65)	520 (217)	(0.16, 0.05)	0.73 (1.03)
15QXF	10.4 (9.0)	257 (79)	306 (128)	(0.16, 0.08)	0.25 (0.35)
25QXF	8.7 (6.9)	193 (55)	250 (105)	(0.16, 0.06)	0.44 (0.64)
33QXF	9.8 (8.4)	356 (186)	270 (210)	(0.16, 0.06)	0.19 (0.30)
50QXF	10.0 (8.4)	250 (102)	240 (130)	(0.16, 0.08)	0.25 (0.34)

[a] The values in parentheses correspond to those for maximum EQE. [b] The CIE coordinates are calculated at the maximum EQE.

Using a thin PVK buffer layer (15 nm), we made two sets of devices of the type ITO/PEDOT/PVK/polymer/cathode, one with pure Al as the cathode (type I) and the other with LiF/Al serving as the electron-injecting electrode (type II). The relevant device parameters of type I and type II LEDs are summarized in Tables 4 and 5, respectively. Figure 7 shows the normalized EL spectra of type II LEDs based on PFO and the QXF copolymers. Expectedly, almost identical EL spectra were observed for the type I LEDs (not shown). The only major difference between the two types of devices is that the operating voltages of type II LEDs are much lower than those of type I LEDs as noted from Tables 4 and 5. Although some interlayer mixing is bound to occur at the PVK/polymer interface due to common solubility in the spin-coating solvent (toluene), the EL spectra of the LEDs are similar to the thin film PL spectra of the corresponding copolymers (Figure 5b). The EL spectra of Figure 7 clearly show that the EL emission stays blue at all operating voltages of the devices for all the QXF copolymers. The CIE coordinates[25] of the EL emission of the QXF copolymers do not vary with operating voltage and are identical to those of the deep-blue EL from PFO homopolymer at ~(0.16, 0.07).

The current density−voltage (J−V) and luminance−voltage (L−V) characteristics of type I LEDs (no LiF layer) are shown in parts a and b, respectively, of Figure 8. The turn-on voltages (voltage at which EL emission is visible to the eye) for the homopolymer PFO diode and the copolymer LEDs are comparable at ~6.0 V. There is no discernible variation in the turn-on voltage with copolymer composition to suggest that electron injection is significantly enhanced in the QXF copolymers containing n-type quinoxaline moieties. LEDs based on 25QXF, 33QXF, and 50QXF showed current spikes in the region below the turn-on voltages. The fact

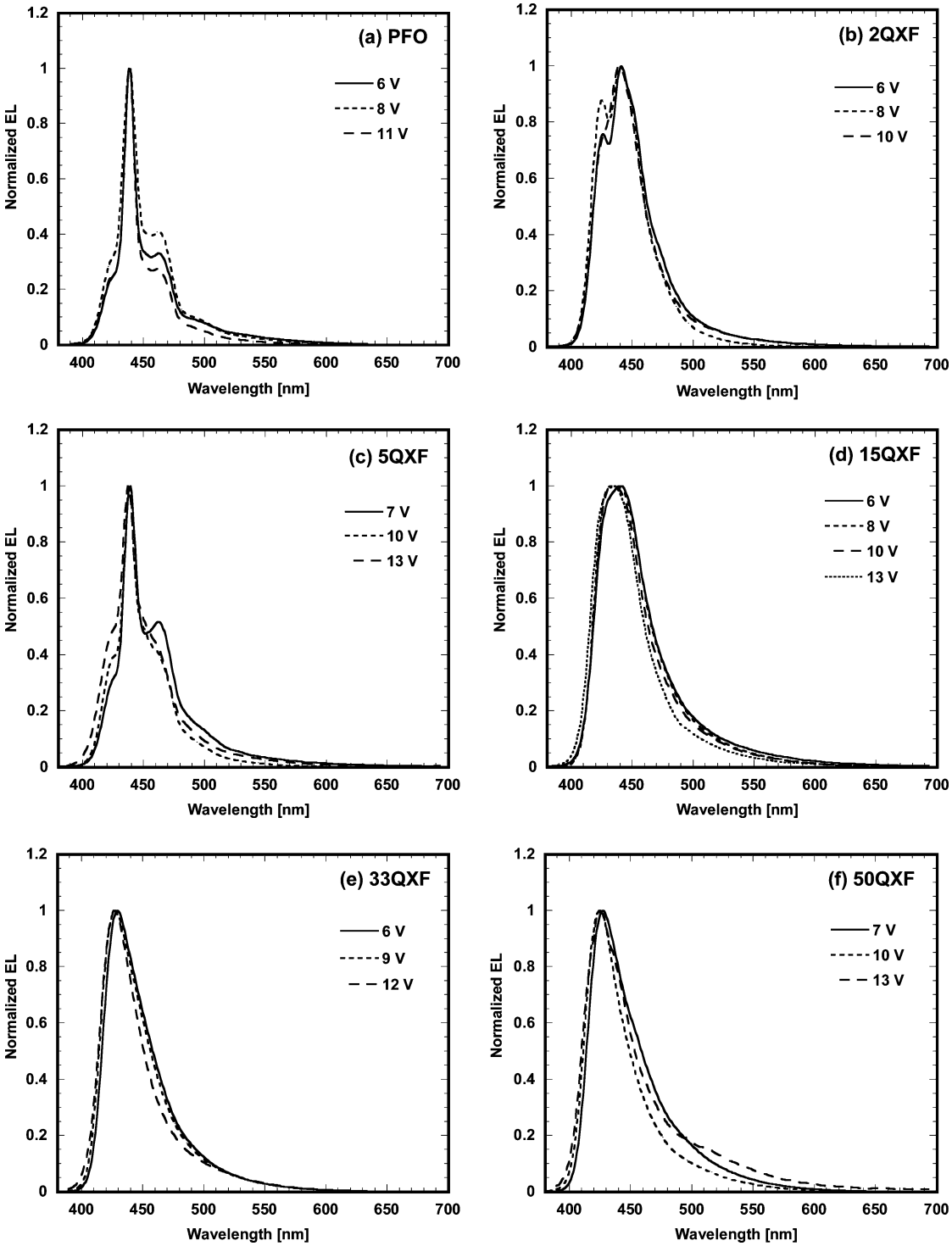

Figure 7. Normalized EL spectra of LEDs of the type ITO/PEDOT/PVK/polymer/LiF/Al: (a) PFO, (b) 2QXF, (c) 5QXF, (d) 15QXF, (e) 33QXF, and (f) 50QXF.

that such spikes are not observed for the copolymers containing lower quinoxaline contents suggests that they could be associated with the filling of interface states or trap states related to the quinoxaline moieties.[26] The traps could be associated with structural defects in the copolymer backbone caused by the kinked quinoxaline linkages. Figure 8b shows the variation in brightness of the type I LEDs as a function of the applied voltage. The PFO homopolymer diode had a maximum brightness of 190 cd/m^2 at 15.6 V and a maximum EQE of 0.053% (500 mA/cm^2, 190 cd/m^2) (Table 4). The best performance among the copolymers was given by 5QXF with a brightness of 560 cd/m^2 at 16.4 V and maximum EQE of 0.35% (500 mA/cm^2, 560 cd/m^2). Copolymer devices with quinoxaline fraction greater than 15 mol % had very low brightnesses and EQEs. For example, the 50QXF copolymer diode had a low brightness of 2 cd/m^2 and a poor EQE of 0.002%. Thus, the device performance varied significantly with quinoxaline content in the copolymers. These results clearly show that composition is in fact a very powerful tool to optimize the properties of electroluminescent copolymers. An alternating copolymer may not necessarily be the optimum composition; superior properties could be achieved from the same building blocks at more dilute copolymer compositions.

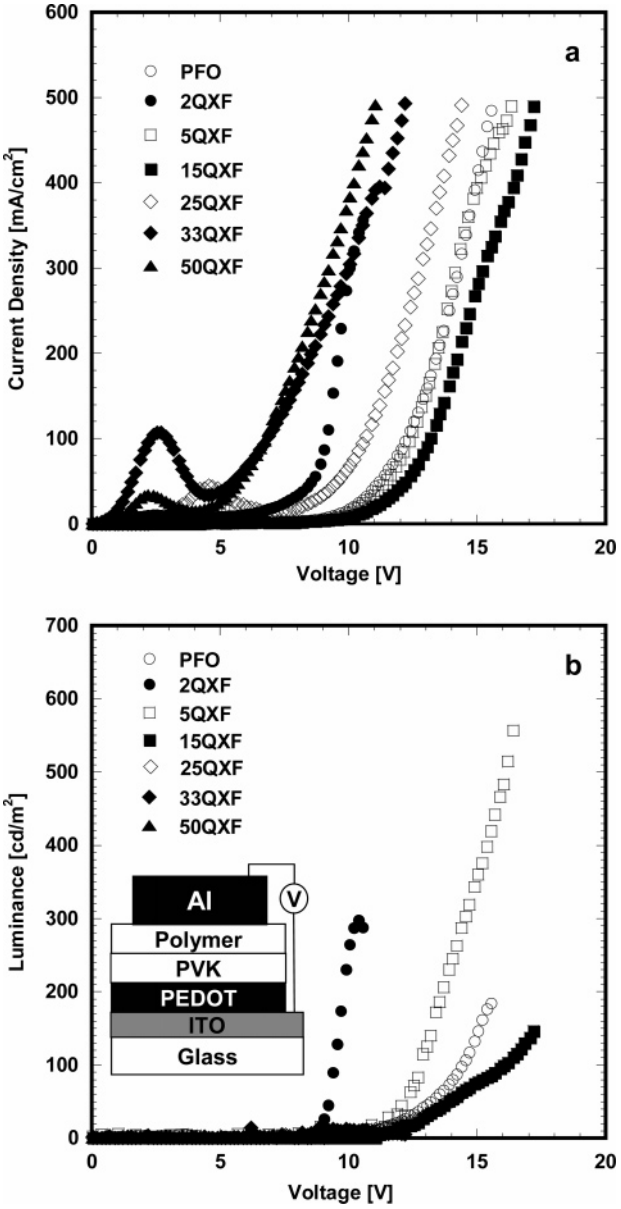

Figure 8. (a) Current density−voltage characteristics of type I polymer LEDs. (b) Luminance−voltage characteristics of the LEDs in (a). The inset shows a schematic of the device.

Parts a and b of Figure 9 show the current density−voltage ($J-V$) and luminance−voltage ($L-V$) characteristics of type II LEDs (with a LiF layer), respectively. Since the overall film thickness of the PVK/polymer bilayer is comparable in all the LEDs, the applied voltage and the electric field are equivalent. The turn-on voltage for the PFO homopolymer diode and the copolymer LEDs is lower at ∼4.5 V, and the operating voltages are lower by ∼3−5 V. It is well-known that LiF enhances electron injection from the cathode and leads to lower turn-on and drive voltages.[27] Superior performance was obtained in the type II LEDs at lower operating voltages as expected. The PFO homopolymer diode had a maximum brightness of 360 cd/m^2 at 8.7 V and maximum EQE of 0.60% (7.1 V, 106 cd/ m^2). The maximum brightness of the 2QXF copolymer LED is slightly lower at 330 cd/m^2, while the best performance is given by 5QXF with a brightness of 520 cd/m^2 at 10.5 V and maximum EQE of 1.03% (9.0 V, 217 cd/m^2). This represents enhancement in performance by a factor of less than 2 compared to that of the PFO homopolymer.

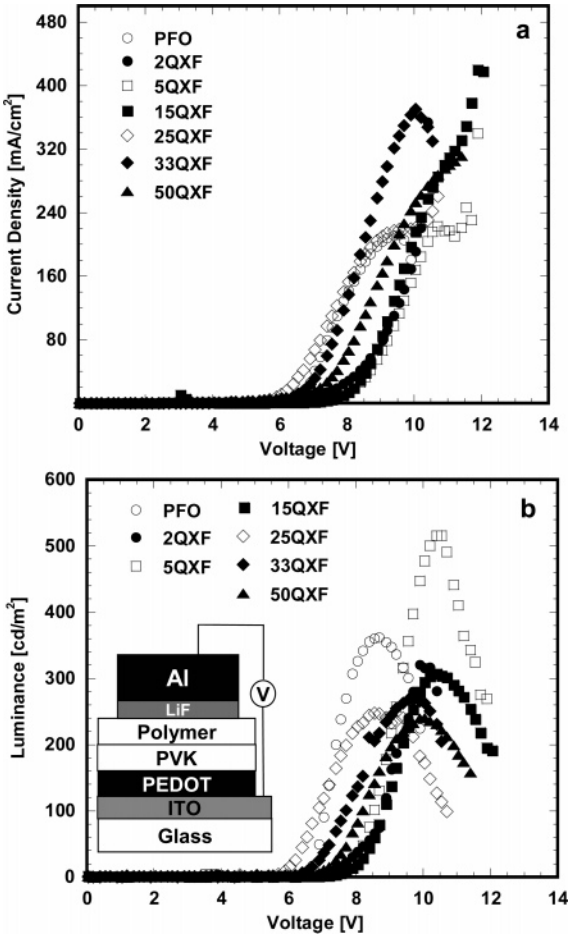

Figure 9. (a) Current density−voltage characteristics of type II polymer LEDs. (b) Luminance−voltage characteristics of the LEDs in (a). The inset shows a schematic of the device.

Nonetheless, the observed device performance is better than or comparable to that of the best blue-emitting polymer LEDs based on polyfluorenes.[9,12] Copolymer LEDs containing greater than 5% quinoxaline had lower brightnesses and EQEs than the PFO device.

The variations in the maximum luminance and EQE of both type I and type II LEDs with quinoxaline content in the copolymer are shown in parts a and b, respectively, of Figure 10. Given that the PL quantum yields of the copolymers decrease steadily with increasing quinoxaline content, the observed variation in the performance for type I LEDs would not be surprising. Both the brightness and the EQE drop significantly with increasing quinoxaline content from 5 to 50 mol %. Enhancement in performance by factors of 3−6 compared to that of PFO is seen for 5QXF, most likely due to a balance in charge carrier injection and transport. However, the variation in performance for type II LEDs is completely different from that for type I LEDs. The best LED performance was still obtained from 5QXF with a maximum EQE of 1% as shown in Figure 10b. In copolymers containing greater than 5 mol % quinoxaline, the brightness and EQE do not drop off significantly as in the type I LEDs. In fact, enhancements in brightness by factors of 2, 4, 23, and 120 are seen for type II LEDs based on 15QXF, 25QXF, 33QXF, and 50QXF, respectively, compared to type I devices. The most likely explanation is the reduction in cathode-induced fluorescence quenching sites at the cathode/polymer interface.[28] It is well-known that thermal evaporation of Al on PFO films leads to covalent Al−C

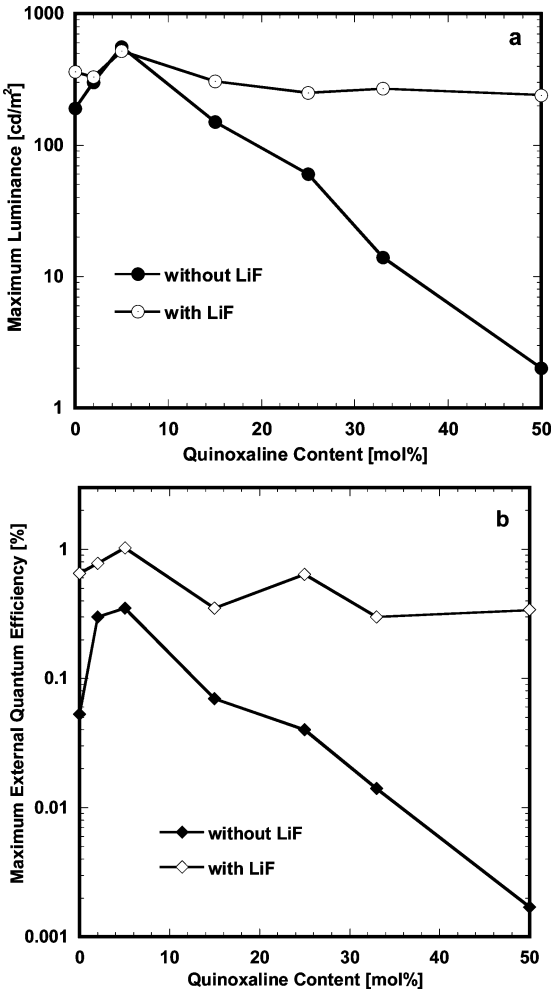

Figure 10. Semilogarithmic plot of maximum (a) luminance and (b) external quantum efficiency of polymer LEDs versus quinoxaline content in the copolymer.

bond formation, disrupting the π-conjugation along the PFO backbone.[28a] We believe that, in the present QXF copolymers, the evaporated Al metal has specific interactions with the quinoxaline moieties in addition to the dioctylfluorene units. Hence, the relative enhancements in brightness and EQE for each type II LED increase with increasing quinoxaline content in the copolymers. The insertion of a thin LiF film between the Al layer and the copolymer presumably prevents the chemical reaction by acting as a barrier layer. Hence, the brightness of the LEDs stays sufficiently high even though the PL quantum yields of the copolymers decrease steadily in going from 5QXF to 50QXF. These results suggest that the incorporation of such thin LiF layers could help enhance the performance of LEDs based on other n-type emissive materials such as polyquinolines[2,3a,b] or anthrazolines[3c] by acting as a buffer. The slight decrease in LED performance of 33QXF or 50QXF compared to PFO is offset by the much improved resistance to thermal oxidation of the QXF copolymers over the PFO homopolymer (Figure 5c). Under continued applied voltage, the copolymer LEDs based on 33QXF or 50QXF will likely not develop the green fluorenone EL emission band, thereby rendering stable blue EL. Overall, the present quinoxaline−fluorene copolymers are promising robust blue electroluminescent materials for LEDs.

Conclusions

A series of five random copolymers and one alternating copolymer of 9,9′-dioctylfluorene and 2,3-bis(*p*-phenylene)quinoxaline were synthesized and successfully used as blue-emitting materials in polymer LEDs. Systematic variations in the polymer properties were seen such as a steady increase in the glass transition temperature from 67 to as high as 160 °C and a decrease in fluorescence quantum yield from 72% to 26% with increasing quinoxaline content from 2 to 50 mol % in the copolymers. The copolymers emit blue light both in dilute solution (417−423 nm) and in the solid state (429−439 nm). Time-resolved fluorescence decay analysis gave short lifetimes of 308−617 ps in both dilute solution and thin films, with no significant interchain aggregation. Blue electroluminescence with CIE coordinates of (0.16, 0.06) and varying performance was achieved from copolymer LEDs of the type ITO/PEDOT/PVK/copolymer/cathode, both with and without a LiF buffer layer, with maximum luminances of 240−520 cd/m^2 and external quantum efficiencies of up to 1% at brightnesses over 100 cd/m^2. Our results showed that the copolymer containing 5 mol % 2,3-bis(*p*-phenylene)-quinoxaline had a significant enhancement in electroluminescence compared to either the PFO homopolymer or any other copolymer. These results clearly demonstrate that composition is a powerful synthetic tool to optimize the electroluminescent properties of light-emitting copolymers. The improved thermal oxidative stability of the quinoxaline-containing copolymers suggests that the fluorene−quinoxaline copolymers are promising materials for stable blue polymer LEDs.

Acknowledgment. This research was supported by the Air Force Office of Scientific Research (Grant F49620-03-1-0162) and the Army Research Office TOPS MURI (Grant DAAD19-01-1-0676).

References and Notes

(1) Reviews: (a) Friend, R. H.; Gymer, R. W.; Holmes, A. B.; Burroughes, J. H.; Marks, R. N.; Taliani, C.; Bradley, D. D. C.; Dos Santos, D. A.; Brédas, J. L.; Lögdlund, M.; Salaneck, W. R. *Nature* **1999**, *397*, 121. (b) Bernius, M. T.; Inbasekaran, M.; O'Brien, J.; Wu, W. *Adv. Mater.* **2000**, *12*, 1737. (c) Kraft, A.; Grimsdale, A. C.; Holmes, A. B. *Angew. Chem., Int. Ed.* **1998**, *37*, 402. (d) Millard, I. S. *Synth. Met.* **2000**, *111−112*, 119. (e) Wu, W.; Inbasekaran, M.; Hudack, M.; Welsh, D.; Yu, W.; Cheng, Y.; Wang, C.; Kram, S.; Tacey, M.; Bernius, M.; Fletcher, R.; Kiszka, K.; Munger, S.; O'Brien, J. *Microelectron. J.* **2004**, *35*, 343. (f) Kulkarni, A. P.; Tonzola, C. J.; Babel, A.; Jenekhe, S. A. *Chem. Mater.* **2004**, *16*, 4556.

(2) (a) Zhang, X.; Shetty, A. S.; Jenekhe, S. A. *Macromolecules* **1999**, *32*, 7422. (b) Jenekhe, S. A.; Zhang, X.; Chen, X. L.; Choong, V.-E.; Gao, Y.; Hsieh, B. R. *Chem. Mater.* **1997**, *9*, 409. (c) Zhang, X.; Jenekhe, S. A. *Macromolecules* **2000**, *33*, 2069. (d) Tonzola, C. J.; Alam, M. M.; Jenekhe, S. A. *Adv. Mater.* **2002**, *14*, 1086.

(3) (a) Zhu, Y.; Alam, M. M.; Jenekhe, S. A. *Macromolecules* **2002**, *35*, 9844. (b) Zhu, Y.; Alam, M. M.; Jenekhe, S. A. *Macromolecules* **2003**, *36*, 8958. (c) Tonzola, C. J.; Alam, M. M.; Kaminsky, W.; Jenekhe, S. A. *J. Am. Chem. Soc.* **2003**, *125*, 13548. (d) Alam, M. M.; Jenekhe, S. A. *Chem. Mater.* **2002**, *14*, 4775.

(4) (a) Liao, L.; Pang, Y.; Ding, L.; Karasz, F. E. *Macromolecules* **2001**, *34*, 7300. (b) Peng, Z.; Bao, Z.; Galvin, M. E. *Chem. Mater.* **1998**, *10*, 2086.

(5) (a) Neher, D. *Macromol. Rapid Commun.* **2001**, *22*, 1365. (b) Scherf, U.; List, E. J. W. *Adv. Mater.* **2002**, *14*, 477. (c) Becker, S.; Ego, C.; Grimsdale, A. C.; List, E. J. W.; Marsitzky, D.; Pogantsch, A.; Setayesh, S.; Leising, G.; Müllen, K. *Synth. Met.* **2002**, *125*, 73.

(6) (a) Redecker, M.; Bradley, D. D. C.; Inbasekaran, M.; Woo, E. P. *Appl. Phys. Lett.* **1998**, *73*, 1565. (b) Babel, A.; Jenekhe, S. A. *Macromolecules* **2003**, *36*, 7759.
(7) (a) Bliznyuk, V. N.; Carter, S. A.; Scott, J. C.; Klärner, G.; Miller, R. D.; Miller, D. C. *Macromolecules* **1999**, *32*, 361. (b) List, E. J. W.; Guentner R.; Scanducci de Freitas, P.; Scherf, U. *Adv. Mater.* **2002**, *14*, 374. (c) Lupton, J. M.; Craig, M. R.; Meijer, E. W. *Appl. Phys. Lett.* **2002**, *80*, 4489. (d) Panozzo, S.; Vial, J.-C.; Kervella, Y.; Stéphan, O. *J. Appl. Phys.* **2002**, *92*, 3495. (e) Gong, X.; Iyer, P. K.; Moses, D.; Bazan, G. C.; Heeger, A. J.; Xiao, S. S. *Adv. Funct. Mater.* **2003**, *13*, 325. (f) Kulkarni, A. P.; Kong, X.; Jenekhe, S. A. *J. Phys. Chem. B* **2004**, *108*, 8689.
(8) (a) Vak, D.; Chun, C.; Lee, C. L.; Kim, J.-J.; Kim, D.-Y. *J. Mater. Chem.* **2004**, *14*, 1342. (b) Lin, W.-J.; Chen, W.-C.; Wu, W.-C.; Niu, Y.-H.; Jen, A. K.-Y. *Macromolecules* **2004**, *37*, 2335. (c) Craig, M. R.; de Kok, M. M.; Hofstraat, J. W.; Schenning, A. P. H. J.; Meijer, E. W. *J. Mater. Chem.* **2003**, *13*, 2861.
(9) (a) Kulkarni, A. P.; Jenekhe, S. A. *Macromolecules* **2003**, *36*, 5285. (b) Sainova, D.; Miteva, T.; Nothofer, G.; Scherf, U.; Glowacki, I.; Ulanski, J.; Fujikawa, H.; Neher, D. *Appl. Phys. Lett.* **2000**, *76*, 1810. (c) Weinfurtner, K.-H.; Fujikawa, H.; Tokito, S.; Taga, Y. *Appl. Phys. Lett.* **2000**, *76*, 2502.
(10) (a) Donat-Bouillud, A.; Levesque, I.; Tao, Y.; D'Iorio, M.; Beaupre, S.; Blondin, P.; Ranger, M.; Bouchard, J.; Leclerc, M. *Chem. Mater.* **2000**, *12*, 1931. (b) Hou, Q.; Zhou, Q.; Zhang, Y.; Yang, W.; Yang, R.; Cao, Y. *Macromolecules* **2004**, *37*, 6299. (c) Kong X.; Kulkarni A. P.; Jenekhe, S. A. *Macromolecules* **2003**, *36*, 8992.
(11) Liu, B.; Yu, W.-L.; Lai, Y.-H.; Huang, W. *Chem. Mater.* **2001**, *13*, 1984.
(12) (a) Wu, F.-I.; Reddy, S.; Shu, C.-F.; Liu, M. S.; Jen, A. K.-Y. *Chem. Mater.* **2003**, *15*, 269. (b) Zhan, X.; Liu, Y.; Wu, X.; Wang, S.; Zhu, D. *Macromolecules* **2002**, *35*, 2529. (c) Yang, W.; Huang, J.; Liu, C.; Niu, Y.; Hou, Q.; Yang, R.; Cao, Y. *Polymer* **2004**, *45*, 865.
(13) (a) Sun, Q.; Zhan, X.; Yang, C.; Liu, Y.; Li, Y.; Zhu, D. *Thin Solid Films* **2003**, *440*, 247. (b) Jung, S. H.; Suh, D. H.; Cho, H. N. *Polym. Bull.* **2003**, *50*, 251.
(14) Yamamoto, T.; Sugiyama, K.; Kushida, T.; Inoue, T.; Kanbara, T. *J. Am. Chem. Soc.* **1996**, *118*, 3930.
(15) (a) Fukuda, T.; Kanbara, T.; Yamamoto, T.; Ishikawa, K.; Takezoe, H.; Fukuda, A. *Appl. Phys. Lett.* **1996**, *68*, 2346. (b) O'Brien, D.; Weaver, M. S.; Lidzey, D. G.; Bradley, D. D. C. *Appl. Phys. Lett.* **1996**, *69*, 881. (c) Cui, Y.; Zhang, X.; Jenekhe, S. A. *Macromolecules* **1999**, *32*, 3824.
(16) Karastatiris, P.; Mikroyannidis, J. A.; Spiliopoulos, I. K.; Kulkarni, A. P.; Jenekhe, S. A. *Macromolecules* **2004**, *37*, 7867.
(17) Heinrich, G.; Schoof, S.; Gusten, H. *J. Photochem.* **1974**, *3*, 315.
(18) Grell, M.; Bradley, D. D. C.; Inbasekaran, M.; Woo, E. P. *Adv. Mater.* **1997**, *9*, 798.
(19) Ahn, T.; Jang, M. S.; Shim, H.-K.; Hwang, D.-H.; Zyung, T. *Macromolecules* **1999**, *32*, 3279.
(20) Jenekhe, S. A.; Lu, L.; Alam, M. M. *Macromolecules* **2001**, *34*, 7315.
(21) Grell, M.; Bradley, D. D. C.; Ungar, G.; Hill, J.; Whitehead, K. S. *Macromolecules* **1999**, *32*, 5810.
(22) Teetsov, J.; Fox, M. A. *J. Mater. Chem.* **1999**, *9*, 2117.
(23) (a) Jenekhe, S. A.; Osaheni, J. A. *Science* **1994**, *265*, 765. (b) Osaheni, J. A.; Jenekhe, S. A. *Macromolecules* **1994**, *27*, 739.
(24) Peisert, H.; Knupfer, M.; Zhang, F.; Petr, A.; Dunsch, L.; Fink, J. *Appl. Phys. Lett.* **2003**, *83*, 3930.
(25) The CIE 1931 coordinates were calculated from the EL spectra on the basis of the standard observer functions taken from Wyszecki, G.; Stiles, W. S. *Color Science: Concepts and Methods, Quantitative Data and Formulae*; Wiley: New York, 1967.
(26) Campbell, A. J.; Bradley, D. D. C.; Lidzey, D. G. *J. Appl. Phys.* **1997**, *82*, 6326.
(27) Brown, T. M.; Cacialli, F. *J. Polym. Sci., Part B: Polym. Phys.* **2003**, *41*, 2649.
(28) (a) Greczynski, G.; Fahlman, M.; Salaneck, W. R. *J. Chem. Phys.* **2000**, *113*, 2407. (b) Stoessel, M.; Wittmann, G.; Staudigel, J.; Steuber, F.; Blassing, J.; Roth, W.; Klausmann, H.; Rogler, W.; Simmerer, J.; Winnacker, A.; Inbasekaran, M.; Woo, E. P. *J. Appl. Phys.* **2000**, *87*, 4467.

MA048118D